TIME DOMAIN MODELING OF EDDY CURRENT EFFECTS FOR TRANSFORMER TRANSIENTS

Francisco de Leon* Adam Semlyen

Department of Electrical Engineering
University of Toronto
Toronto, Ontario, Canada, M5S 1A4

* On leave from Instituto Politecnico Nacional, Mexico

Abstract. - Eddy current effects have been included in the model of the transformer for the study of electromagnetic transients. Existing analytical formulas for the calculation of losses in the windings have been evaluated. Various equivalent circuits have been fitted to represent in the time domain the damping produced by eddy currents in the windings. A frequency dependent model has been derived for the iron core, based on the physical distribution of losses and magnetization effects. The parameters of this model are obtained by optimal discretization of the laminations. Simulations of transients have been presented to show the effects of eddy currents in the damping of transients.

Keywords: Eddy currents, Transformer modeling, Electromagnetic transients.

INTRODUCTION

The global eddy current problem in a transformer includes the eddy currents in the windings, in the core and in the tank. In this paper we deal with the first two. In relation to the eddy current effects in transformer windings, only frequency domain results [1]-[6] are available at present. In the paper we describe methodologies for the synthesis of lumped parameter circuits that adequately represent the eddy current effects in the windings and iron core of a transformer for the study of electromagnetic transients. These models are derived by fitting electric circuits to the analytical expressions for the impedance of windings and laminations. The impedance equations for the windings are the complex extension of already existing expressions for the eddy current losses, obtained by the solution of the electromagnetic field problem (Maxwell's equations) with different assumptions about the field geometry. We achieve an accurate representation of the effects of eddy currents up to very high frequencies with relatively low order models.

The equivalent circuits derived for the representation of eddy currents in the windings and in the iron core are intended to be used, in conjunction with our previous work on transformer modeling [7],[8], in a complete transformer model for the study of electromagnetic transients. The accurate modeling of eddy current effects is very important for predicting the damping during transients since the actual resistance of the windings at high frequencies is by several orders of magnitude larger than its low frequency value and the penetration depth into the laminations at high frequencies is very small.

There are two physical phenomena that occur simultaneously in the windings of a transformer:

- *skin effect*, the non-uniform distribution of the current in a conductor (with a corresponding increase in losses) due to the magnetic field produced by the current in the conductor itself, and
- *proximity effect*, the non-uniform distribution of the current in a conductor (with a still larger increase in losses) due to the magnetic field produced by the current in neighboring conductors.

The two phenomena are usually calculated together and the overall non-uniform distribution of the current in the conductors of a transformer is called *eddy current effect in the windings*. Both this and the time domain modeling of the *eddy current effect in the laminations* will be discussed in the following sections.

92 WM 251-9 PWRD A paper recommended and approved by the IEEE Transformers Committee of the IEEE Power Engineering Society for presentation at the IEEE/PES 1992 Winter Meeting, New York, New York, January 26-30, 1992. Manuscript submitted January 29, 1991; made available for printing January 22, 1992.

ANALYTICAL FORMULATION OF EDDY CURRENT EFFECTS

Traditionally, Maxwell's equations for the study of eddy currents are formulated for the quasi-static electromagnetic field. These formulations yield diffusion equations that can be solved analytically using simplified geometries. The resulting expressions are generally acceptable for the analysis of the behavior of electric machines. Designers, however, are not always satisfied with their accuracy and often rely on numerical solutions (for example finite elements) for more realistic geometries.

Windings

There exists a number of analytical expressions for the calculation of losses in the transformer windings [1]-[6]. As we are interested not only in the losses produced by the eddy currents but also in the magnetic effects, we derive in this paper expressions for the impedance. The basic assumptions made in the derivations are:

a) The magnetic field has only an axial component, parallel to the axis of the windings.

b) The conductors have a rectangular cross section.

c) All conductors carry the same total current. This precludes the consideration of parallel conductors and sets a limit in the maximum frequency of validity for the equations.

d) There is no gap between conductors (see Figure 1). However, the surface field intensity is assumed to be undisturbed by the eddy currents.

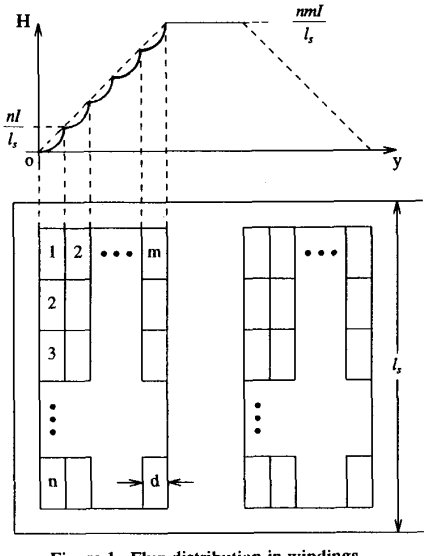

Figure 1. Flux distribution in windings

These assumptions imply that the magnetic field at the lateral surfaces of the conductors is known and it can be used to specify the boundary conditions. Thus we have a distribution of the magnetic field intensity as illustrated in Figure 1. This distribution is different from the well known trapezoidal distribution of the magnetic field in that we allow for a non uniform field distribution inside the conductors.

Solution for Infinitely Long Conductors

If in addition to the basic assumptions we assume that the length of the conductors is infinite (or that their curvature is zero), then the eddy current problem for each conductor is reduced to a one-dimensional diffusion equation in cartesian coordinates. A step-by-step solution of this boundary value problem can be found in references [4] and [5] for the losses in each layer of the winding. We use a similar approach to obtain the impedance as a function of frequency (see Appendix A). The impedance for a conductor in layer k is given (in Ω/m) by

$$Z_w(\omega) = R_w\, \xi\, [\, (2k^2-2k-1)\coth(\xi) - 2k(k-1)\,\mathrm{csch}(\xi)\,] \qquad (1)$$

where

$$R_w = \frac{1}{\sigma\, l_s\, d} \qquad \xi = \sqrt{j\,\omega\,\mu\,\sigma}\; d$$

Solution Considering the Curvature of the Conductors

In this case, the problem is reduced to the solution of a field problem in one dimension in cylindrical coordinates. The step-by-step solution for the losses can be found in reference [5] and is very similar to the derivation of equation (1) when using the asymptotic expansions for large arguments in the Bessel (Kelvin) functions (see Appendix B). The final expression for the impedance of a conductor in layer k (in Ω) is

$$Z_w(\omega) = 2\,\pi\, R_w\, \xi\, [\, (k^2 r_k + (k-1)^2 r_{k-1})\coth(\xi) - 2k(k-1)\sqrt{r_k\, r_{k-1}}\;\mathrm{csch}(\xi)\,] \qquad (2)$$

There are a number of other different approaches. For example, in reference [2] Stafl solves the problem considering that the field can vary in the perpendicular direction inside the conductors (two dimensions), while keeping the boundary conditions as in the previous cases, when the length of the conductors is infinite. This leads to a solution given by an infinite series. In reference [3] the problem is solved as in the case of reference [2] (two dimensions), but taking into consideration the radius of curvature.

In this paper we selected the axisymmetric approach (equation (2)) to be consistent with the way in which we calculated the inductances and capacitances in reference [7], where we used axisymmetric geometry. The last two approaches mentioned above were not considered for the fitting of circuits because the resulting infinite series have numerical problems at high frequencies (see reference [4]). The infinite series converge very slowly and the accuracy of these approaches is comparable to the one obtained with equation (1). Moreover, the simplicity of equations (1) and (2) is a very convenient and desirable feature that will be exploited for the low frequency fitting of equivalent circuits.

Analytical approaches may be used for the calculation of the total loss and the a.c./d.c. resistance ratio. However, these equations do not predict properly the location of the hot spots. These conclusions were drawn from comparisons of the results from the analytical equations with measurements and numerical solutions (see [4]). In reference [5], Figure 2-9, the real part of the equation (1) is compared with measurements. This test proves that the real part of equation (1) predicts with reasonable accuracy the resistance of a series connected winding. A comparison between equations (1) and (2) was also presented. There is no significant difference between them for realistic coils but, since the derivation of equation (2) uses a more realistic geometry while having the same simplicity, we selected the latter as our basis for the calculation of the impedance of the windings as a function of frequency.

Iron Core

The field problem in the iron core has been understood for many years and the solutions can be found, for example, in references [6] and [9]. The impedance of a lamination is given by:

$$Z_l(\omega) = R_l\, \xi \tanh(\xi) \qquad (3)$$

where

$$R_l = \frac{2\,w}{\sigma\, l\, d} \qquad \xi = \sqrt{j\,\omega\,\mu\,\sigma}\; d \qquad (3a)$$

and

l = length of the lamination
w = with of the lamination
$2\,d$ = thickness of the lamination

LUMPED PARAMETER MODELS

In this section we will derive equivalent circuits with lumped parameters from different fitting techniques. We do the fitting to equation (2) for the windings and to equation (3) for the iron core.

Windings

We use Foster models to describe the frequency dependence of the windings (increase of resistance with frequency). Foster models are usually referred to as circuits obtained from the expansion of impedance (or admittance) equations into partial fractions which are fitted by canonical R, L, C circuits [10]. The Foster models obtained in this way would have to be of infinite order to reproduce exactly the impedance at all frequencies. The terms (or circuit blocks) that have to be omitted for practical reasons will produce errors over the whole frequency spectrum. The errors increase with the frequency range for a fixed model order. The same kind of circuits can however be obtained by fitting only at certain pre-established frequencies using an iterative method. These circuits would have the exact impedance at the selected frequencies, while the response will not be perfect at other frequencies. The latter approach gives smaller overall errors and will therefore be adopted in this paper.

We can fit a circuit using any one of the two Foster forms:

a) The *parallel Foster* that, in our case, consists of series R-L blocks connected in parallel (see Figure 2);

b) The *series Foster* that consists of parallel R-L blocks, connected in series (see Figure 3).

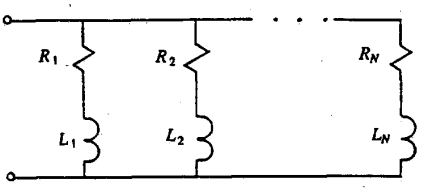

Figure 2. Parallel Foster

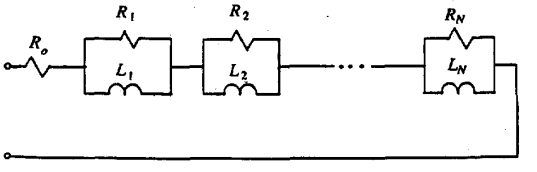

Figure 3. Series Foster

Parallel Foster

The admittance Y_{pF} at the terminals of the parallel Foster circuit shown in Figure 2 is given by

$$Y_{pF}(\omega) = \sum_{i=1}^{N} \frac{1}{R_i + j\,\omega\, L_i} \qquad (4)$$

We can evaluate equations (2) and (4) at N frequencies ω_k ($\omega_{k+1} > \omega_k$) and derive a system of nonlinear equations which permits the calculation of the parameters of the circuit (R_i and L_i). We use a fixed point iteration starting with the highest frequency. Thus, equation (4) yields

$$Y_{pF}(\omega_k) = \sum_{i=1}^{N} Y_i(\omega_k) = \frac{1}{Z_w(\omega_k)} = Y_w(\omega_k) \qquad (k = N,\ldots,2,1) \qquad (5)$$

Extracting the kth term from the sum of equation (5) gives

$$Y_k(\omega_k) = Y_w(\omega_k) - \sum_{\substack{i=1 \\ i \neq k}}^{N} Y_i(\omega_k) \qquad (k = N,\ldots,2,1) \qquad (6)$$

Consequently,

$$R_k = \mathrm{Re}\left[\frac{1}{Y_k(\omega_k)}\right] \qquad (k = N,\ldots,2,1) \tag{7}$$

and

$$L_k = \frac{1}{\omega_k}\,\mathrm{Im}\left[\frac{1}{Y_k(\omega_k)}\right] \qquad (k = N,\ldots,2,1) \tag{8}$$

We use equations (7) and (8) iteratively to update all R_k and L_k until we achieve convergence.

Series Foster

The series Foster form has advantages over the parallel Foster at low frequencies as discussed below. We will present several versions of the series Foster that have advantages over the standard Foster.

Complex Fitting

The impedance at the terminals of the series Foster circuit shown in Figure 3 is given by

$$Z_{sF}(\omega) = R_o + \sum_{i=1}^{N} \frac{\mathrm{j}\,\omega L_i R_i}{R_i + \mathrm{j}\,\omega L_i} \tag{9}$$

As in the case of the parallel Foster we evaluate equation (9) at N frequencies to obtain the parameters of the circuit. Using the kth frequency to get the kth inductance and resistance we have

$$\frac{1}{R_k} - \mathrm{j}\,\frac{1}{\omega_k L_k} = \frac{1}{Z_w(\omega_k) - R_o - \sum_{\substack{i=1 \\ i\neq k}}^{N} \frac{\mathrm{j}\,\omega_k L_i R_i}{R_i + \mathrm{j}\,\omega_k L_i}} \qquad (k = N,\ldots,2,1) \tag{10}$$

The right hand side of equation (10) is evaluated numerically and then its real and imaginary parts give R_k and L_k. We note that, upon convergence, both the real and the imaginary parts of the circuit match the corresponding parts of the prescribed impedance (2). This model will be called *series complex* to differentiate it from other series forms described below.

Real-Only Fitting

The internal impedance of the conductors is given by equation (2). This is just one of the two components that form the total leakage impedance

$$Z_{leak} = Z_w + Z_{air} \tag{11}$$

The impedance for the air path has only imaginary part, and its magnitude is much larger than the imaginary part of equation (2). Therefore, there is no need to fit a circuit to accurately match the imaginary part of equation (2) since this component in the total impedance is only of minor importance. Consequently, we propose to fit the parameters of the series Foster to twice as many frequencies (as in the complex model for the same number of parameters) to match only the real part of the impedance, without any fitting for the imaginary part. We could have done the same for the parallel Foster but, as we will show later, the series circuits have advantages over the parallel ones at low frequencies. In this way, we have a lower order model that matches the real part accurately at the fitting frequencies and, as we will show below, the inductance does not have large errors. From equation (9),

$$R_{sF}(\omega) = \mathrm{Re}[\,Z_{sF}(\omega)\,] = R_o + \sum_{i=1}^{N} \frac{\omega^2 L_i^2 R_i}{R_i^2 + \omega^2 L_i^2} = \mathrm{Re}\,[\,Z_w(\omega)\,] \tag{12}$$

Extracting the kth block from equation (12) yields

$$\frac{\omega^2 L_k^2 R_k}{R_k^2 + \omega^2 L_k^2} = a(\omega) \tag{13}$$

where

$$a(\omega) = \mathrm{Re}\,[\,Z_w(\omega)\,] - R_o - \sum_{\substack{i=1 \\ i\neq k}}^{N} \frac{\omega^2 L_i^2 R_i}{R_i^2 + \omega^2 L_i^2}$$

Evaluating (13) at two frequencies, ω'_k and ω''_k, we have, with $a'_k = a(\omega'_k)$ and $a''_k = a(\omega''_k)$,

$$\frac{\omega'^2_k L_k^2 R_k}{R_k^2 + \omega'^2_k L_k^2} = a'_k \qquad (k = N,\ldots,2,1) \tag{13a}$$

and

$$\frac{\omega''^2_k L_k^2 R_k}{R_k^2 + \omega''^2_k L_k^2} = a''_k \qquad (k = N,\ldots,2,1) \tag{13b}$$

Equations (13a) and (13b) form a system of two equations of second order with two unknowns (R_k and L_k). There exists closed form solution for equations (13) given by

$$R_k = \frac{a'_k a''_k (\omega''^2_k - \omega'^2_k)}{a'_k \omega''^2_k - a''_k \omega'^2_k} \qquad (k = N,\ldots,2,1) \tag{14a}$$

and

$$L_k = \frac{a'_k \omega''^2_k - a''_k \omega'^2_k}{(a''_k - a'_k)\,\omega'^2_k \omega''^2_k} R_k \qquad (k = N,\ldots,2,1) \tag{14b}$$

Equations (14) are used iteratively to update the elements of the circuit until convergence is reached.

Osculatory Fitting

When we want a very accurate response at low frequencies (up to a few kHz) we can sacrifice one R-L block to perform an osculatory fitting of the real part of the impedance equation. The term "osculatory" denotes in differential geometry a contact of two curves having equal curvatures in the point of contact.

The Taylor expansion for the transcendental functions in equation (2) are [11],[12]

$$\xi\coth(\xi) = 1 + \frac{\xi^2}{3} - \frac{\xi^4}{45} + \frac{2\,\xi^6}{945} - \frac{\xi^8}{4725} + \cdots \tag{15a}$$

$$\xi\,\mathrm{csch}(\xi) = 1 - \frac{\xi^2}{6} + \frac{7\,\xi^4}{360} - \frac{31\,\xi^6}{15120} + \frac{127\,\xi^8}{604800} - \cdots \tag{15b}$$

Recall that ξ is a function of $\sqrt{\mathrm{j}}$ and, as we are only interested in the real part of the impedance, we keep only the terms with ξ^0, ξ^4 and ξ^8 in the above expressions. The resulting resistance is obtained by substituting equations (15) in equation (2) and adding all the layers:

$$R_c(\omega) = a_o + a_4\,\omega^2 + a_8\,\omega^4 + \cdots \tag{16}$$

where

$$a_o = [\,F_1 + F_2\,] \qquad a_4 = \left[\frac{F_1}{45} - \frac{7\,F_2}{360}\right]\mu^2\,\sigma^2\,d^4$$

$$a_8 = \left[-\frac{F_1}{4725} + \frac{127\,F_2}{604800}\right]\mu^4\,\sigma^4\,d^8$$

$$F_1 = (2\,\pi\,R_w)\sum_{k=1}^{n} k^2 r_k + (k-1)^2 r_{k-1} \qquad F_2 = -2\,(2\,\pi\,R_w)\sum_{k=1}^{n} k(k-1)\sqrt{r_k\,r_{k-1}}$$

On the other hand, from equation (9) for the circuit of Figure 2 we have the following Taylor series (when $\omega \to 0$)

$$R_{sF}(\omega) = R_o + \sum_{i=1}^{N}\left(\frac{L_i^2}{R_i}\right)\omega^2 - \sum_{i=1}^{N}\left(\frac{L_i^4}{R_i^3}\right)\omega^4 + \cdots \tag{17}$$

Comparing equations (16) and (17) we have

$$R_o = a_o \tag{18a}$$

$$\sum_{i=1}^{N}\frac{L_i^2}{R_i} = a_4 \tag{18b}$$

$$\sum_{i=1}^{N}\frac{L_i^4}{R_i^3} = -a_8 \tag{18c}$$

Using equations (18b) and (18c) we can obtain the closed form solutions

$$R_1 = \frac{c_1^2}{c_2} \qquad L_1 = \sqrt{c_1\,R_1} \tag{19}$$

where

$$c_1 = a_4 - \sum_{i=2}^{N} \frac{L_i^2}{R_i} \qquad c_2 = -a_8 - \sum_{i=2}^{N} \frac{L_i^4}{R_i^3}$$

In this case the first block of the real-only fitting is changed for an osculatory one. Thus, we use in the iterative cycle equations (14) for $k = N, \ldots, 3, 2$ and equations (19) for $k = 1$.

Results and Discussion

Our first remark pertains to the differences between the two Foster forms (series and parallel). The series Foster form is obtained from impedance equations and is more suitable for low frequencies. Note, for example, the appearance of a zero order block R_o at the beginning of the circuit. This is the low frequency (or d.c.) resistance. The parallel Foster form is derived from admittance equations so that a leading, purely resistive branch would represent the resistance at infinite frequency. Thus, in order to have a similar response at the lower part of the frequency spectrum, the parallel Foster has to be of an order higher by one than the series Foster. Indeed, in the parallel Foster we will have to sacrifice one of the branches to fit at zero (or near zero) frequency, while in the series Foster this is naturally taken into account by R_o. For a more detailed discussion see reference [10].

The convergence of the described iterative fitting methods does not present any problem if the fitting frequencies are sufficiently apart from each other. In this way, each block is of dominant significance at its fitting frequency (or frequencies) and it is almost isolated from the other blocks during the iterative process. Based on the experience gained in [13] and [14] we start the fitting iteration at the highest frequency. In this way we get convergence in just a few iterations, less than 10 in most cases. The circuits were tested using a real (small) transformer, described in Appendix 2 of reference [7]. The selection of the fitting frequencies was done heuristically; no optimization of the errors for a given frequency range was pursued. In Figure 4 we show the errors in the resistance as a function of frequency (up to 1 MHz). The three series Foster models are compared against the real part of equation (2). Figure 4a corresponds to models of order three with fitting frequencies given in Table 1, while Figure 4b shows the errors of a circuit of order 4. We can see from Figure 4 that the error is zero at the fitting frequencies (as expected) while at other frequencies there is an error which decreases considerably for a model of order 4 in comparison with a model of order 3.

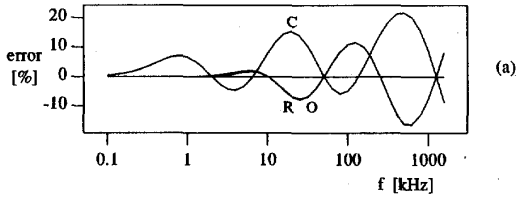

Models of order 3

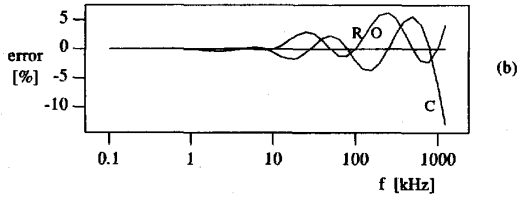

Models of order 4

Figure 4. Variation of resistance with frequency
C - Complex, R - Real-only, O - Osculatory

MODEL	ORDER 3 Frequencies [kHz]	ORDER 4 Frequencies [kHz]
COMPLEX	2, 50, 1250	0.8, 8, 80, 800
REAL-ONLY	0.4, 2, 10, 50, 250, 1250	0.5, 1, 5, 10, 50, 100, 500, 1000
OSCULATORY	10, 50, 250, 1250	5, 10, 50, 100, 500, 100

Table 1. Fitting frequencies

We also see from Figure 4 that the real-only fitting models are superior to the series complex Foster. The real-only and osculatory models are almost equivalent. The choice between the two could be based on the frequency range in which we are interested. The best low frequency response is achieved with the osculatory model, but we sacrifice two frequencies. If we are more interested in higher frequencies, the real-only model would be the choice, since it makes possible to fit at higher frequencies. In Figure 5 we show the frequency response of the resistance (with R_o subtracted) corresponding to the osculatory model of order 4. The plot shows (as expected) an almost quadratic response at low frequencies and a square root response at high frequencies (both given by the slope in the log-log plot).

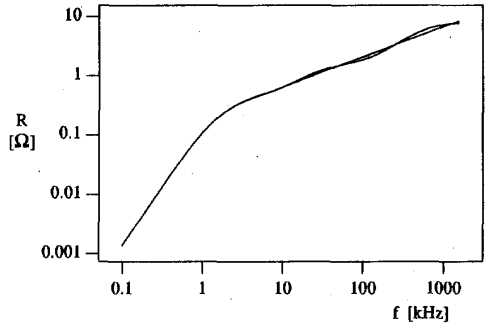

Figure 5. Variation of resistance with frequency
$R(\omega) - R_o$

In spite of the fact that the imaginary part of the real-only fittings is not constrained, and thus it could take any value, we can see from Figure 6a that the inductance as a function of frequency is also very accurate. The reason for such a good response is that the errors (which may be large) are introduced in a small component (the internal inductance) compared with the total leakage inductance. The errors in the calculation of the internal inductance are small at low frequencies, where they could be important since at zero frequency the magnetic field completely penetrates the conductors. At high frequencies the errors in the calculation of the internal inductance are large (100% or more) but, as this component of the total leakage inductance decreases quickly to almost zero, the net effect of those large errors is very small. In Figure 6b, we show the frequency response of the total leakage inductance (for the case described before) where we can appreciate the size of the two components.

The criterion we suggest for selecting the order of the model, according to the maximum frequency we are interested in, is shown in Table 2. This table was obtained heuristically to keep the errors within reasonable limits.

No. of Blocks	0	1	2	3	4
Frequency [kHz]	0.1	1	10	100	1000

Table 2. Selection of the model order

Iron Core

There exists a standard Cauer model for laminations, obtained by developing equation (3) in continued fractions. The resulting equivalent circuit has shunt inductances and series resistances forming a ladder [10]. However, this Cauer model cannot be interpreted as a discretization of the lamination and it predicts accurately the terminal response only in the linear case. Another form of a Cauer model (a more physical approach) would have shunt resistances and series inductances [15]; see Figure 7. The inductances represent (using duality) the flux paths and the resistances are in the path of the eddy currents. This a dual of the standard Cauer circuit but it cannot be derived directly from equation (3). The high frequency response is defined by the blocks near the terminals (as the magnetic field in the laminations stays near the surface at high frequencies), while in the standard Cauer circuit, the high frequency behavior is governed by the inner blocks. The blocks of our model can

be thought of as being a discretization of the lamination. This model is appropriate for the representation of nonlinear effects inside the lamination.

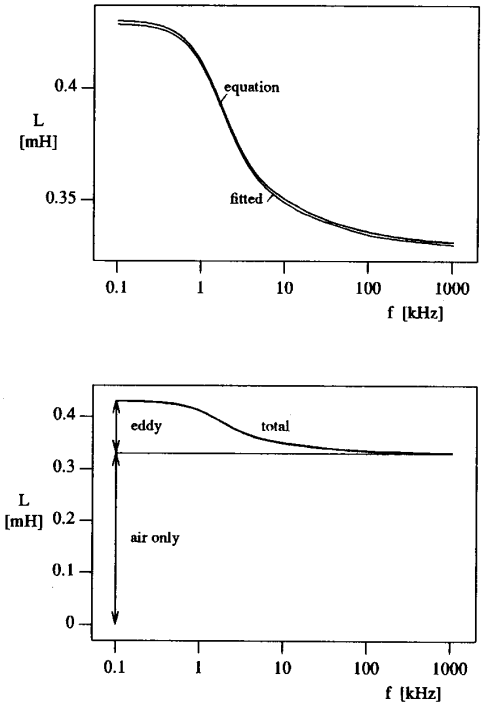

Figure 6. Variation of inductance with frequency at two vertical scales

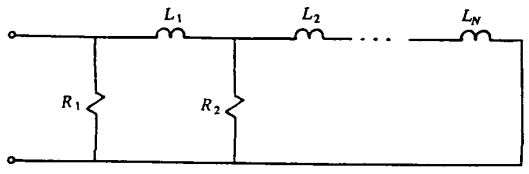

Figure 7. Cauer model for half lamination

The parameters of this physical Cauer circuit will be calculated with an iterative method. The iterative method could be seen as an optimization of the discretizing distances for the used fitting frequencies. The impedance at the terminal of the circuit shown in Figure 7 is given by

$$Z_C(\omega) = \cfrac{1}{G_1 + \cfrac{1}{j\omega L_1 + \cfrac{1}{G_2 + \cdots \cfrac{1}{G_N + \cfrac{1}{j\omega L_N}}}}} \tag{20}$$

To start the iterative method we estimate initial values for all the parameters and, as in the previous cases, we start with the highest frequency. Assume that we are calculating the elements of the kth block. The impedance at $\omega = \omega_k$ seen at the right of block k is

$$Z_{kR} = \cfrac{1}{G_{k+1} + \cfrac{1}{j\omega_k L_{k+1} + \cfrac{1}{G_{k+2} + \cdots \cfrac{1}{G_N + \cfrac{1}{j\omega_k L_N}}}}} \tag{21}$$

The impedance at the left of the block is

$$Z_{kL} = \cfrac{1}{-G_{k-1} + \cfrac{1}{-j\omega_k L_{k-1} + \cfrac{1}{-G_{k-2} + \cdots \cfrac{1}{-G_1 + \cfrac{1}{Z_l(\omega_k)}}}}} \tag{22}$$

Looking into block k we have

$$Z_{kL} = \frac{1}{G_k + \cfrac{1}{j\omega_k L_k + Z_{kR}}} \qquad (k = 1,2,...,N-1) \tag{23}$$

Equation (23) has G_k and L_k as unknowns. It will be modified for computing the elements (G_k and L_k) of the first $N-1$ blocks, while for the last one (the innermost) we will use the osculatory conditions for G_N and L_N.

Rearranging equation (23) we have

$$\frac{1}{Z_{kL}} = G_k + \frac{1}{j\omega_k L_k + Z_{kR}} \qquad (k = 1,2,...,N-1) \tag{24}$$

Let $Z_{kR} = R_{kR} + j\omega_k L_{kR}$. We can separate the real and imaginary parts of (24) as follows:

$$\mathrm{Re}\left[\frac{1}{Z_{kL}}\right] = G_k + \frac{R_{kR}}{R_{kR}^2 + (\omega_k L_k + \omega_k L_{kR})^2} = a \qquad (k = 1,2,...,N-1) \tag{25a}$$

$$\mathrm{Im}\left[\frac{1}{Z_{kL}}\right] = -\frac{\omega_k L_k + \omega_k L_{kR}}{R_{kR}^2 + (\omega_k L_k + \omega_k L_{kR})^2} = -b \qquad (k = 1,2,...,N-1) \tag{25b}$$

From equation (25b) we can write the quadratic equation for $\omega_k L_k + \omega_k L_{kR}$

$$b\,(\omega_k L_k + \omega_k L_{kR})^2 - (\omega_k L_k + \omega_k L_{kR}) + b\,R_{kR}^2 = 0 \qquad (k = 1,2,...,N-1) \tag{26}$$

Its solution gives directly L_k (since L_{kR} is known), for $k = 1,2,...,N-1$, and then G_k, using equation (25a).

The equations for the last (innermost) block are obtained in a way that ensures a good (osculatory) behavior at low frequencies. Expanding $\xi \tanh(\xi)$ in equation (3) into the truncated Taylor series [11], [12]

$$\xi^2 - \frac{\xi^4}{3}$$

and substituting the values of ξ and R_l from equation (3a), gives the expression of the impedance at $\omega \to 0$:

$$Z_l(\omega) \approx j\omega L_{dc} + \omega^2 L_{dc}^2 G_{dc} \tag{27}$$

where

$$L_{dc} = \mu \frac{2wd}{l} \qquad G_{dc} = \frac{1}{3R_l} \tag{28}$$

The definition of G_{dc} is in agreement with the definition of R_{dc} in reference [9]. We note that equation (27) represents the impedance at $\omega \to 0$ of a parallel $G_{dc} - L_{dc}$ circuit. Therefore, the last (innermost) inductance of the ladder can be obtained from

$$L_N = L_{dc} - \sum_{k=1}^{N-1} L_k \tag{29}$$

For the calculation of the last conductance G_N we consider the voltage divider formed by the series inductances at $\omega \to 0$ (when the current in the shunt conductances is negligible compared with the current in the inductances) and move each conductance G_k to the terminals, with the equivalent value

$$G'_k = \frac{\sum_{i=k}^{N} L_i}{\sum_{i=1}^{N} L_i} G_k$$

Consequently, G_N can be calculated from

$$G_N = \left(\frac{\sum_{i=1}^{N} L_i}{L_N}\right)\left(G_{dc} - \sum_{k=1}^{N-1} G'_k\right) \tag{30}$$

The calculation of the parameters consists of the iterative solution of equations (26) for the first $N-1$ blocks and equations (29) and (30) for the last one.

We have also performed real-only fitting (even though its justification is not easy) but the results obtained were not as good as in the case of the windings. Therefore, the details of the related methodology are not discussed in this paper.

Results and Discussion

We have compared the frequency response of our model with equation (3). Table 3 shows the data and maximum errors for several orders of the model up to a frequency of 200 kHz.

Model Order	F [kHz]	Error (resistance) [%]	Error (inductance) [%]
3	0 40 170	5.3	6.3
4	0 13 40 180	0.88	0.74

Table 3. Maximum errors up to 200 kHz

The frequency response (up to 1 MHz) of a model of order 5 is presented in Figure 8. The fitting frequencies in this case are 0, 20, 60, 350 and 1000 kHz. Figure 8a presents the resistance and Figure 8b the inductance, and we can see that the fitting is excellent. The errors in percent are shown in Figure 9. As we can see from Figure 9 the errors at the fitting frequencies are zero. The errors in the resistance and inductance are smaller than 1% over the whole frequency range.

Note that in equation (3) and, consequently, in the parameters of our model the variables ω and μ always appear in the product form $\omega\mu$. Therefore, the frequency responses presented here are valid for any degree of saturation by simply scaling the frequency axis to keep the product $\omega\mu$ constant.

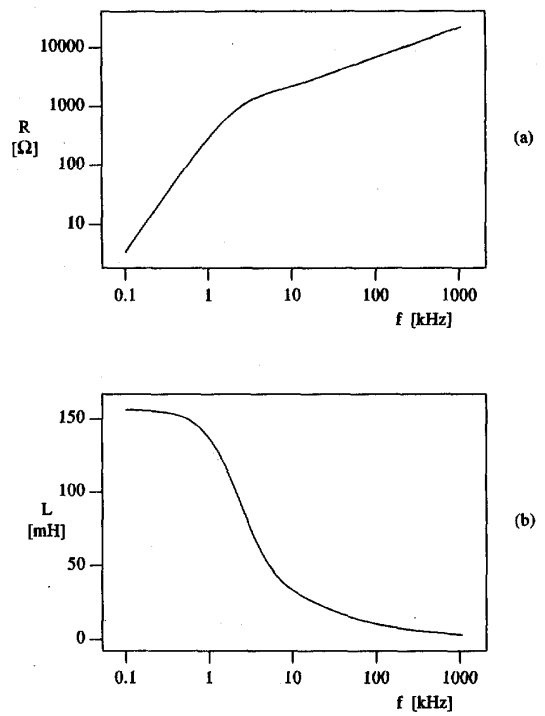

Figure 8. Variation of R and L with frequency

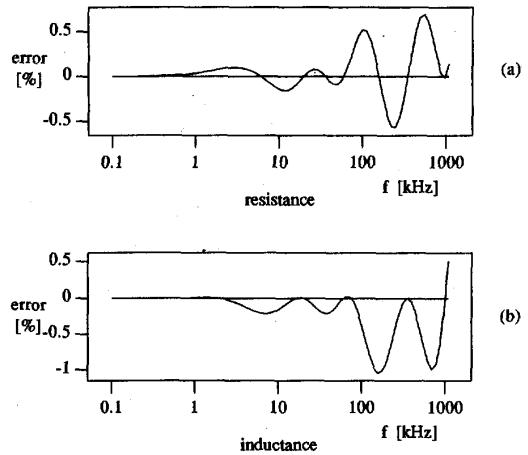

Figure 9. Variation of resistance and inductance with frequency Model of order 5

SIMULATION TESTS

Two tests were designed to show the damping effect of the eddy currents during transient conditions. The data used for both tests corresponds to the small transformer described in Appendix 2 of reference [7]. The first test consists of the interruption of the short circuit current following a short circuit test. The primary voltage is, therefore, small and the magnetizing current negligible. This test is deemed to assure appropriate conditions where the effect of eddy currents in the windings is of paramount importance in determining the attenuation of fast transients. In the simulation we used the series Foster model of Figure 3 together with a series capacitance. An oscillating voltage is obtained due to the leakage inductance and the stray capacitances. Figure 10 shows the results of the simulation. We note that, as expected, there is considerably greater damping when the eddy current effects in the windings are included. The time constant ($2\,L_{leak} / R_o$) when the eddy current effects are neglected is 19.25 ms ($L_{leak} = 4.3 \times 10^{-4}$ H, $R_o = 0.0447\ \Omega$). From Figure 10 we can see that the time constant when the eddy current effects are considered is $\approx 120\ \mu$s. The frequency of oscillation ($f \approx 1 / (2\,\pi\,\sqrt{L_{leak}\,C}\,)$) with $C = 1 \times 10^{-10}$ F is $f = 767$ kHz. Test results on a 450 MVA, 339/138 kV, 3-phase autotransformer given in Figure 8 of reference [16] show that the measured attenuation is of the same order of magnitude as the one we have obtained in Figure 10 in the simulation of eddy current effects.

The second test is the simulation of chopping a magnetizing current. In this case the oscillation is between the stray capacitances and the magnetizing inductance. This test provides conditions for demonstrating the dominant effect of the modeling of eddy currents in laminations on the nature and attenuation of a transient response. For this simulation we have used the Cauer model of Figure 7 with a shunt capacitance at its terminals. Figure 11a corresponds to an overdamped response and steep front, for the case of a small capacitance. We require a model of order 5 or 6 to properly predict the eddy current effects in the laminations. The underdamped response is shown in Figure 11b. It corresponds to a larger capacitance. For this case a model of order 4 would be adequate. The order of the model is obviously dependent on the speed of the transient we are interested in.

The complete analytical solution for both tests was obtained using eigenanalysis. In the case of the windings we found only one pair of complex conjugate eigenvalues with the attenuation and frequency of oscillation in agreement with the results obtained in the simulation of Figure 10. The remaining eigenvalues are real and the corresponding modes attenuate faster than for the complex pair. Moreover, from the initial conditions we found that these modes are practically not excited. This confirms the absence of d.c. components in the simulated transients. Similarly, in the case of the iron core the analytical solutions corroborate the simulated results of Figure 11.

The tests have demonstrated the significance of eddy current modeling in both the windings and the laminations for obtaining more realistic results, especially in terms of damping, in the simulation of transformer transients.

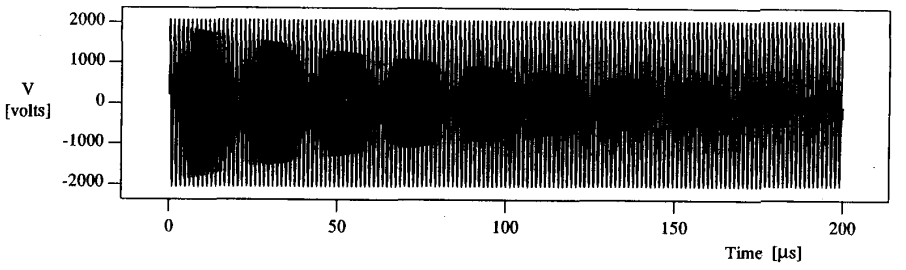

Figure 10. Short circuit current chopping.
Low frequency model vs model of order 4

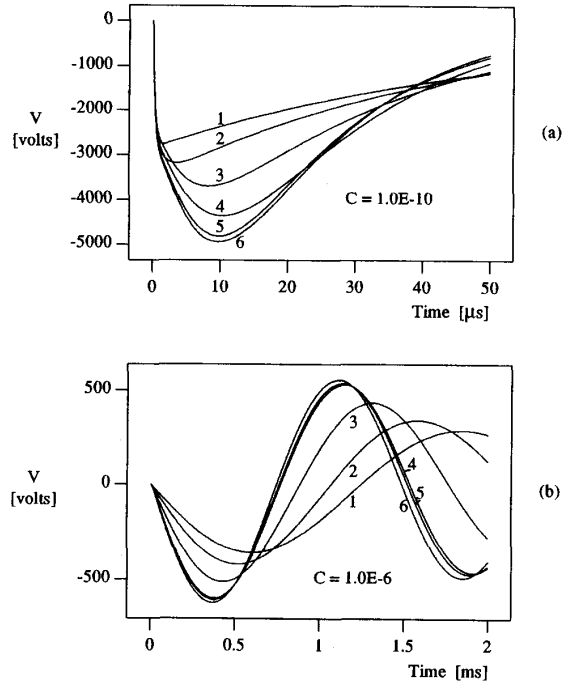

Figure 11b. Magnetizing current chopping.
Models orders 1 to 6

CONCLUSIONS

Time domain models have been derived for the representation of eddy current effects of transformers in the windings and in the iron core.

For the windings we have the following remarks:

Existing (and well tested) equations for the calculation of eddy current losses in transformer windings were used in their impedance form to fit different lumped parameter models. These models have a series Foster form and their order has been reduced by fitting to the real part only. The low frequency response is optimized by osculatory fitting.

For the iron core we note the following:

A dual Cauer model has been derived with optimal discretization of the laminations thickness. This model predicts very accurately the variation of the resistance and inductance as a function of frequency.

Tests performed with the new models for eddy current representation have shown that they provide appropriate damping effects in the simulation of transients as determined by the underlying physical phenomena.

The lumped parameter models presented in this paper can be incorporated in a complete transformer model for the calculation of transients.

ACKNOWLEDGEMENTS

Financial support by the Natural Sciences and Engineering Research Council of Canada is gratefully acknowledged. The first author wishes to express his sincere gratitude to the National Council of Science and Technology of Mexico (CONACYT) and to the National Polytechnic Institute of Mexico for the financial support of his studies at the University of Toronto.

REFERENCES

[1] W. Rogowski, "Über zusätzliche Kupferverluste, über die kritische Kupferhöhe einer Nut und über das kritische Widerstandsverhältnis einer Wechselstrommaschine", Archiv für Electrotechnik, Volume II, No. 3, pp. 81-118, 1913.

[2] M. Stafl, "Electrodynamics of Electrical Machines", Academia, Publishing House of the Czechoslovak Academy of Sciences, Praga 1967.

[3] J. Lammeraner and M. Stafl, "Eddy Currents", The Chemical Rubber Co. Press, Cleveland, 1966.

[4] K. Gallyas, "Current Density and Power Loss Distribution in Sheet Windings", Ph.D. Thesis, University of Toronto, 1975.

[5] M. Perry, "Low Frequency Electromagnetic Design", Marcel Dekker, Inc., 1985.

[6] R. Stoll, "The Analysis of Eddy Currents", Clarendon Press, Oxford, 1974.

[7] F. de Leon and A. Semlyen, "Efficient Calculation of Elementary Parameters of Transformers", paper no. 91 WM 002-6 PWRD presented at the 1991 IEEE/PES Winter Meeting.

[8] F. de Leon and A. Semlyen, "Reduced Order Model for Transformer Transients", paper no. 91 WM 126-3 PWRD presented at the 1991 IEEE/PES Winter Meeting.

[9] J. Avila-Rosales and F. Alvarado, "Nonlinear Frequency Dependent Transformer Model for Electromagnetic Transient Studies in Power Systems", IEEE Transactions on Power Apparatus and Systems, Vol. PAS-101, No. 11, November 1982.

[10] L. Weinberg, "Network Analysis and Synthesis", McGraw-Hill, 1962.

[11] Staff of Research and Education Association, "Handbook of mathematical, Scientific, and Engineering Formulas, Tables, Functions, Graphs, Transforms", Research and Education Association, 1984.

[12] M. R. Spiegel, "Mathematical Handbook", McGraw-Hill, 1968.

[13] A. Semlyen and A. Deri, "Time Domain Modelling of Frequency Dependent Three-Phase Transmission Line Impedance", IEEE Transactions on Power Apparatus and Systems, Vol. PAS-104, No. 6, June 1985, pp. 1549-1555.

[14] W. Wei-Gang and A. Semlyen, "Computation of Electro-Magnetic Transients on Three-Phase Transmission Lines with Corona and Frequency Dependent Parameters", IEEE Transactions on Power Delivery, Vol. PWRD-2, No. 3, July 1987, pp. 887-898.

[15] J. Avila-Rosales and A. Semlyen, "Iron Core Modelling for Electrical Transients", IEEE Transactions on Power Apparatus and Systems, Vol. PAS-104, No. 11, November 1985, pp. 3189-3194.

[16] R.J. Musil, G. Preininger, E. Schopper, and S. Wenger, "The Resonance Effect of Oscillating System Overvoltages on Transformer Windings", IEEE Transactions on Power Apparatus and Systems, Vol. PAS-101, No. 10, October 1982, pp. 3703-3711.

APPENDICES

Appendix A. Solution for Infinitely Long Conductors

As shown in reference [5], it is possible to find the solution of the boundary value problem of equation (A-1) for the calculation of the losses. Our purpose is, however, to derive the expression (1) of the complex impedance $Z_n(\omega)$. We start with the diffusion equation in one dimension (see Figure 1 for the geometry) given by

$$\frac{d^2 h_z(y)}{d y^2} = \alpha^2 h_z \tag{A-1}$$

where

$$\alpha^2 = j\,\omega\,\mu\,\sigma$$

with boundary conditions

$$h_z(-\frac{d}{2}) = (k-1)H_s, \quad h_z(\frac{d}{2}) = k H_s \tag{A-2}$$

and

$$H_s = \frac{n I}{l_s}$$

The general solution is

$$h_z(y) = K_1 e^{\alpha y} + K_2 e^{-\alpha y} \tag{A-3}$$

The constants are evaluated from the boundary conditions which yields

$$K_1 = \frac{(k-1)H_s e^{-\frac{\alpha d}{2}} - kH_s e^{\frac{\alpha d}{2}}}{e^{-\alpha d} - e^{\alpha d}} \tag{A-4a}$$

$$K_2 = \frac{kH_s e^{-\frac{\alpha d}{2}} - (k-1)H_s e^{\frac{\alpha d}{2}}}{e^{-\alpha d} - e^{\alpha d}} \tag{A-4b}$$

Substituting equations (A-4) into (A-3), we get after some algebraic steps

$$h_z(y) = kH_z \frac{\cosh(\alpha y)}{\cosh(\frac{\alpha d}{2})} + H_z \frac{\sinh(\alpha y - \frac{\alpha d}{2})}{\sinh(\frac{\alpha d}{2})} \tag{A-5}$$

From

$$\frac{d\,h_z(y)}{d\,y} = \sigma\, e_x(y) \tag{A-6}$$

we have

$$e_x(y) = \frac{kH_z\alpha}{\sigma} \frac{\sinh(\alpha y)}{\cosh(\frac{\alpha d}{2})} + \frac{H_z\alpha}{\sigma} \frac{\cosh(\alpha y - \frac{\alpha d}{2})}{\sinh(\frac{\alpha d}{2})} \tag{A-7}$$

We will compute the surface impedance from the Poynting vector which is defined (in VA/m^2) as

$$\Pi = \frac{1}{2} E \times H^* \tag{A-8}$$

Developing the vector product gives

$$2\,\Pi_x(y) = -e_x(y)\,h_z(y) \tag{A-9}$$

The complex power consumed (in VA) is given by the closed surface integral

$$S = \int \Pi \cdot dS \tag{A-10}$$

In our one dimensional geometry the Poynting vector penetrates perpendicularly into the windings so that the surface integral is calculated in a straightforward fashion. This is in contrast with the volume integrals (for losses) used in references [4] and [5] which are awkward. Equation (A-10) (VA/m) yields

$$S = (\Pi_{in} - \Pi_{out})\, l_s \tag{A-11}$$

where

$$\Pi_{in} = \Pi_x(-\frac{d}{2}) = \frac{H_z^2\,\alpha}{4\,\sigma} [\,(2k^2-3k+1)\tanh(\frac{\alpha d}{2}) + (1-k)\coth(\frac{\alpha d}{2})\,] \tag{A-12}$$

$$\Pi_{out} = \Pi_x(\frac{d}{2}) = -\frac{H_z^2\,\alpha}{2\,\sigma} [\,k^2 \tanh(\frac{\alpha d}{2}) + k\,\mathrm{csch}(\frac{\alpha d}{2})\,] \tag{A-13}$$

Substituting equations (A-12) and (A-13) into (A-11) and reducing terms we get

$$S = \frac{l_s\,H_z^2\,\alpha}{2\,\sigma} [\,(2k^2-2k+1)\coth(\alpha d) - 2k(k-1)\,\mathrm{csch}(\alpha d)\,] \tag{A-14}$$

Substituting H_s and realizing that I is the crest value of the current (this gives a factor of 2), we can obtain the impedance by dividing S by I_{rms}^2. This yields equation (1) of the paper for $n=1$.

Appendix B. Solution Considering the Curvature of the Conductors

We follow very similar steps to the previous case. In reference [5] the problem is solved for the losses. In this case the diffusion equation to be solved is, in cylindrical coordinates,

$$r^2 \frac{d^2 h_z(r)}{d r^2} + r \frac{d\,h_z(r)}{d\,r} - j\,\beta^2 r^2 h_z(r) = 0 \tag{B-1}$$

where

$$\beta^2 = \omega\,\mu\,\sigma$$

with boundary conditions

$$h_z(r_{k-1}) = (k-1)\,H_s, \quad h_z(r_k) = k\,H_s \tag{B-2}$$

Equation (B-1) is a form of the modified Bessel equation of zero order. Its solution is

$$h_z(r) = C_1\,[\,\mathrm{ber}_o(\beta r) + j\,\mathrm{bei}_o(\beta r)\,] + C_2\,[\,\mathrm{ker}_o(\beta r) + j\,\mathrm{kei}_o(\beta r)\,] \tag{B-3}$$

where ber_o, bei_o, ker_o, kei_o are the Kelvin functions of zero order.

The constants C_1 and C_2 can be evaluated from the boundary conditions following a similar procedure as in Appendix A. We use the asymptotic expansions for large arguments of Kelvin functions, as r_k is much larger than d for a realistic transformer. The used substitutions (for $x \gg 1$) are

$$\mathrm{ber}_p(x) \simeq e^{x/\sqrt{2}} \cos(\frac{\phi_p}{\sqrt{2\pi x}}) \quad \mathrm{bei}_p(x) \simeq e^{x/\sqrt{2}} \sin(\frac{\phi_p}{\sqrt{2\pi x}}) \tag{B-4a}$$

$$\mathrm{ker}_p(x) \simeq e^{-x/\sqrt{2}} \cos(\frac{\psi_p}{\sqrt{2\pi/x}}) \quad \mathrm{kei}_p(x) \simeq -e^{-x/\sqrt{2}} \sin(\frac{\psi_p}{\sqrt{2\pi/x}}) \tag{B-4b}$$

where

$$\phi_p = \frac{x}{\sqrt{2}} - \frac{\pi}{8} + \frac{p\,\pi}{2} \quad \psi_p = \frac{x}{\sqrt{2}} + \frac{\pi}{8} + \frac{p\,\pi}{2}$$

Then we can obtain $e_\phi(r)$ by an equation similar to (A-6), taking the derivative of $h_z(r)$. The remaining steps are the same as in the previous case and equation (2) is obtained.

Francisco de Leon (St.M) was born in Mexico City, Mexico, in 1959. He received his B.Sc. degree and his M.Sc. degree (summa cum laude) from the National Polytechnic Institute of Mexico, in 1983 and 1986 respectively. From 1984 to 1987 he was a lecturer at the same institute. Currently, he is working towards his Ph.D. degree at the University of Toronto. His main interests are in the areas of transformer modeling and electromagnetic fields.

Adam Semlyen (F'87) was born and educated in Rumania where he obtained a Dipl. Ing. degree and his Ph.D. He started his career with an electric power utility and held an academic position at the Polytechnic Institute of Timisoara, Rumania. In 1969 he joined the University of Toronto where he is a professor in the Department of Electrical Engineering. His research interests include the steady state and dynamic analysis of power systems, electromagnetic transients, and power system optimization.

Discussion

Cesare M. Arturi (Politecnico di Milano, Italy). I wish to congratulate Professor Semlyen and Dr. de Leon for their very interesting paper on the circuital model of eddy current effects in the windings and the core of transformers.

The subject faced by the authors is very important for the time domain simulation of transients in non sinusoidal operation. The model of eddy current losses in the time domain, due to the load current of transformers, has been studied in the past, particularly for the actual load losses in HVDC transformers windings [1]. An improvement of the series element (actual winding resistances and leakage inductance) of the equivalent network of transformers has also been considered [2].

Thus, the contribution given by the Authors to the mathematical procedure for the iterative determination of the parameters of time domain models suitable for transients with a wide frequency range is highly appreciated.

With reference to the iron core and the physical Cauer model, the parameters of which are obtained by an iterative method with eq.(3), the authors stated that this model is appropriate for the representation of non linear effects inside the laminations. I wonder how the magnetizing characteristics can be assigned to the inductances of the model.

Further, it is not clear to the discusser what the authors intend by the word "dual" when they refer to the relationships between the standard and the physical Cauer model.

I should appreciate it if the authors could comment on these points.

[1] C.M.Arturi, A.Bossi, G.Caprio, A.Babare, S.Calabrò, F. Coppadoro, S.Crepaz, "Conventional and Actual Losses in HVDC Transformers", Cigré, Session 1986, Aug. 27-4 Sept., Paris.

[2] S. Crepaz, M. Ubaldini, "Equivalent networks of transformers and static machines...", Symposium on Power and Measurement Transformers - Positano (Italy), 11-13 Sept. 1979 - p.161-169.

Manuscript received February 20, 1992.

A. Narang, E. P. Dick, (Ontario Hydro, Canada): We wish to congratulate the authors for their work and for a thought-provoking presentation of their results. The paper makes a notable contribution with regard to fitting reduced order models, in this case to classic closed-form solutions describing eddy current effects in windings and in laminations. We would welcome their comments on the following:

1. Equation (1) appears to have a typographical error, as it predicts negative impedance for conductors in the first layer (i.e. for k = 1).

2. Even though expressions (1) and (3) appear dissimilar, incorporating as they do diverse hyperbolic functions, the authors' results confirm that they exhibit similar impedance variation with frequency (compare Figure 5 to 8a, and 7a to 8b). Analytically, this is confirmed by examining the behaviour of the functions over the full range of the argument ξ. This is gratifying as the underlying principle is the same in both instances, whether associated with eddy currents in laminations or in windings. This being the case, it is not clear why different network topologies have been chosen for modeling essentially the same mechanism. The authors correctly point out that the adopted form of the Cauer network permits a physical interpretation for laminations based on duality. As such, iron non-linearities can be introduced in this representation on a physical basis/[a]/, a facility not readily available with Foster realizations. While we accept that such interpretation is not needed for the winding model, nor necessarily meaningful at least for multi-layered windings, do the authors envisage numerical or conceptual advantages in the Foster realization for winding effects?

3. The model for eddy current effects in winding neglects displacement currents, assuming the same total current in each turn. As such, it ought to be valid at frequencies below the first winding resonance (quarter-wave resonance), typically up to perhaps 10's of kHz for power transformers. Is it therefore correct that a model of order 2 or perhaps 3 would be adequate for practical studies? For the example depicted in Figure 10, does clearing a terminal fault produce winding transients at a frequency exceeding the first resonance? If so, the foregoing assumption is no longer valid, and it is not clear whether losses/damping would be over- or under-estimated. Have the authors compared their simulated results with measurements on the cited transformer. How does the simulated 767 kHz transient compare with the winding natural frequency?

Reference

[a] E. J. Tarasiewicz, A. S. Morched, A. Narang, E. P. Dick, "Frequency Dependent Eddy Current Models for NonLinear Iron Cores," Paper No. 92 WM 177-6 PWRS presented at the 1992 IEEE/PES Winter Meeting.

Manuscript received February 26, 1992.

F. de Leon and A. Semlyen (University of Toronto): We would like to thank the discussers for their interest in our paper.

To Professor Arturi we offer the following remarks regarding the physical Cauer model for the laminations. The inductances in the Cauer circuit for the iron-core are derived by discretizing the laminations. Therefore, each inductance corresponds to a subsection of the lamination width. Consequently, the same magnetization characteristic of the material can be used directly in all inductances of the Cauer circuit. The word "dual" was used for the physical Cauer model to indicate that this circuit has series inductances and shunt resistances (Figure 7) as opposed to the standard (non-physical) Cauer model which has shunt inductances and series resistances.

To Messrs. Narang and Dick we offer the following answers to their questions.

1. We thank the discussers for pointing out the *typographical error* in equation (1). The correct expression, consistent with the derivation in Appendix A, follows from equation (A–14) and should be

$$Z_w(\omega) = R_w\, \xi\, [\, (2k^2-2k+1)\coth(\xi) - 2k(k-1)\,\mathrm{csch}(\xi)\,] \qquad (1)$$

We take this opportunity to list below *typographical errors in the two related references*, [7] and [8]. In reference [7], Appendix 2, Figure 8, the thickness of the windings should be 0.7 cm in both primary and secondary.

The following are errors in reference [8]. Below equation (12) we should have

$$\mathbf{v}_a = [\mathbf{v}^T\,,\, e_{y_1}\,]^T = [v_1\,,\, v_2\,,\, \cdots\,,\, v_M\,,\, e_{y_1}\,]^T$$

Equation (21b) should be

$$\sum_{k=1}^{N} w_k\, i_{c_k} - i_{\alpha_c} - i_{\beta_c} + i_{y_2} = 0$$

Below equation (28), matrix **W** should read

$$\mathbf{W} = \begin{bmatrix} \mathbf{w} & & & \\ 1 & & -1 & \\ & \mathbf{w} & & \\ & 1 & 1 & -1 \\ & & \mathbf{w} & \\ & & 1 & 1 \end{bmatrix}$$

The second equation in Appendix 1 of reference [8] should be

$$\mathbf{v}_a^{hist} = \mathbf{v}_a^{old} - \mathbf{w}_a\, e_a^{old} + \mathbf{R}_{TH}\, \mathbf{i}_a^{old}$$

2. There are four commonly used circuits that can be fitted for the time domain representation of eddy currents in laminations and in windings. Namely,
   a) Parallel Foster (Figure 2)
   b) Series Foster (Figure 3)
   c) Standard Cauer (shunt inductances and series resistances; see Figure 5 of the discussers' reference [a])
   d) Dual Cauer (series inductances and shunt resistances; see Figure 7).

   From a physical point of view, model *d* is the most suitable alternative for the modeling of eddy currents in laminations.

   For the time domain representation of eddy current effects in the windings, alternatives *b* and *c* offer practical advantages over alternatives *a* and *d*. The former two allow for leading series resistances which can represent the d.c. resistance of the winding and therefore the order of the models is reduced by one. Alternative *b* was selected in the paper over alternative *c* due to computational advantages, since Foster models lead to simpler state equations than Cauer circuits.

3. We would like to emphasize that, as pointed out by the discussers, the eddy current model should be used with caution. The model can only be used as it is for windings or sections where the current is close to uniform. For a fast transient, such as the one presented in Figure 10, only the order of magnitude of the damping can be predicted as the frequency of the oscillations is above the first resonance frequency of the transformer.

   For the modeling of eddy currents in the windings we have adopted two different approaches. The first one uses several series Foster circuits to include the capacitive effects. In the second approach we use a single series Foster circuit per winding and compute an average current to obtain the correct losses. This latter approach leads to an eddy current representation that can be easily incorporated into any existing transformer model which does not include the damping due to eddy currents. We intend to publish the details of the above two solutions in the near future.

Manuscript received April 9, 1992.